

Review

# Sonoporation, a Novel Frontier for Cancer Treatment: A Review of the Literature

Martina Ricci <sup>1,†</sup> , Elisa Barbi <sup>1,†</sup>, Mattia Dimitri <sup>1</sup> , Claudia Duranti <sup>2</sup> , Annarosa Arcangeli <sup>2,\*</sup>   
and Andrea Corvi <sup>1</sup> 

<sup>1</sup> Department of Industrial Engineering, University of Florence, Via di Santa Marta 3, 50139 Florence, Italy; martina.ricci1@unifi.it (M.R.); elisa.barbi@edu.unifi.it (E.B.); mattia.dimitri@unifi.it (M.D.); andrea.corvi@unifi.it (A.C.)

<sup>2</sup> Department of Experimental and Clinical Medicine, University of Florence, Viale Morgagni 50, 50134 Florence, Italy; claudia.duranti@unifi.it

\* Correspondence: annarosa.arcangeli@unifi.it

† These authors contributed equally to this work.

**Abstract:** Sonoporation has garnered significant attention for its potential to temporarily permeabilize cell membranes through the application of ultrasound waves, thus enabling an efficient cellular uptake of molecules. Despite its promising applications, the precise control of sonoporation remains a complex and evolving challenge in the field of cellular and molecular biology. This review aims to address two key aspects central to advancing our understanding of sonoporation. Firstly, it underscores the necessity for the establishment of a standardized methodology to validate and quantify the successful entry of molecules into target cells. This entails a critical examination of existing techniques and the identification of best practices to ensure accurate, reliable, and reproducible results. By establishing a common framework for assessing sonoporation outcomes, researchers can enhance the reliability and comparability of their experiments, paving the way for more robust findings. Secondly, the review places particular emphasis on the detailed analysis of various acoustic parameters as reported in the papers selected from the literature. Among these parameters, acoustic intensity (specifically, ISPTA) emerges as a pivotal factor in sonoporation studies. Furthermore, this review delves into the exploration of the elastic modulus and its significance in sonoporation mechanisms and associated challenges. This knowledge can inform the development of more effective strategies to optimize sonoporation protocols. In summary, this review not only highlights the pressing need for a standardized approach to verify molecule entry into cells but also delves into the search for an effective frequency and acoustic intensity for in vivo and in vitro applications.

**Keywords:** sonoporation; ultrasound; ISPTA



**Citation:** Ricci, M.; Barbi, E.; Dimitri, M.; Duranti, C.; Arcangeli, A.; Corvi, A. Sonoporation, a Novel Frontier for Cancer Treatment: A Review of the Literature. *Appl. Sci.* **2024**, *14*, 515. <https://doi.org/10.3390/app14020515>

Academic Editor: Maria Filomena Botelho

Received: 23 November 2023

Revised: 27 December 2023

Accepted: 4 January 2024

Published: 6 January 2024



**Copyright:** © 2024 by the authors. Licensee MDPI, Basel, Switzerland. This article is an open access article distributed under the terms and conditions of the Creative Commons Attribution (CC BY) license (<https://creativecommons.org/licenses/by/4.0/>).

## 1. Introduction

Ultrasounds are a widely used tool in diagnostics for the detection of pathologies and also for therapeutic treatments, since they are a less invasive and non-toxic technique producing mechanical, thermal, and biochemical effects.

There are several areas of application of ultrasound in diagnostics, such as Echodoppler, echo color Doppler, and, in the pre-clinic field, the use of ultrasound-guided inoculation in mouse models [1], which allows for more natural tumor growth and less animal suffering.

On the other hand, the main therapeutic areas in which ultrasound is used are lithotripsy, physiotherapeutics with musculoskeletal rehabilitation therapies, and tissue regeneration. One of the areas in which research is focusing, especially for cancer treatment, is ultrasound-induced apoptosis [2,3], which can be divided into the following:

- Low-intensity pulsed ultrasound (LIPUS);
- Low-intensity continuous ultrasound (LICU), related to sonomechanical effects;
- HIFU therapy, a thermal ablation technique.

Furthermore, measurements of the radial temperature field show that enhanced heating effects remain localized. This localized heating effect could have important implications and applications in various fields such as ablation. The HIFU technique holds significant promise, particularly in localized heating effects, with applications in ablation procedures for various medical conditions. Ultrasound's therapeutic potential extends to minimally invasive endoscopic surgery, exemplified by procedures like kidney stone and uterine fibroid removal. Ultrasound waves are utilized to mechanically disrupt these structures while minimizing invasiveness [4,5]. The present article is focused on ultrasound-induced sonoporation, which represents the transient permeabilization of the cell membrane. This process enables the uptake and cellular release of macro- and micro-molecules [6] due to the development of nano- and micrometer-sized pores on the surface. However, it is still a challenge to achieve a controlled and secure opening mechanism due to the lack of real-time monitoring methods; in fact, the mechanisms remain not fully known. This introductory section outlines the two main themes of the paper: the collection of different types of ultrasound verification techniques presented in the various papers selected, or, put another way, determining how the penetration of a molecule into the cell was verified; and then the collection of parameters with a precise *modus operandi* to unify the variables from a methodological and scientific point of view.

### *1.1. The Biological and Physical Mechanisms behind Sonoporation: Standardize the Post-Stimulation Verification Methodology*

The basic principle of ultrasound-induced sonoporation is supposed to be the cavitation effect. During the alternating cycles of rarefaction and compression generated by an ultrasonic field, microbubbles expand and contract repeatedly due to the change in acoustic pressure [7]. At low levels of the latter, the microbubbles exhibit stable cavitation, oscillating with a relatively small amplitude around their balance volume. When, however, the acoustic intensity (ISATA) exceeds a certain threshold, typically  $5 \text{ W/cm}^2$  [8,9], the microbubble collapses forcefully, mechanically breaking the membrane; this effect is called inertial cavitation. Understanding this process is essential for a better understanding of the opening and closing mechanics of the membrane. Real-time verification is a goal to strive for and a research gap to fill; however, the analysis of the literature reveals, for the most part, post-entry verification techniques of the molecule in the cell. Some researchers investigate sonoporation dynamics with voltage clamp techniques, in which changes in transmembrane current under fixed voltage conditions are evaluated, which directly reflect a change in cell membrane conductance, indicating the opening and closing of pores [10]. A comprehensive understanding of microbubbles necessitates a closer examination of their application. The inspiration to utilize microbubbles stems from their established role as contrast agents in the diagnostic application of ultrasound. These bubbles, when introduced into a medium, enhance the visibility of structures during imaging. It is hypothesized that the phenomenon of cavitation, a crucial aspect in this context, is not solely contingent on whether these microbubbles are injected *in situ* or incorporated into an *in vitro* culture. Instead, the cavitation process is believed to be facilitated by the presence of natural gases in the cell.

### *1.2. The US Parameters behind Sonoporation: Correlation between Ultrasound Physics and Mechanical Tissue Variables*

In research on sonoporation, it is necessary to standardize physical and acoustic parameters in correlation with the effectiveness and the types of tissues treated, with particular attention to the following:

- Frequency.
- Acoustic intensity.

The investigation undertaken in the literature places a notable emphasis on the examination of ISPTA as a pivotal component alongside its concomitant parameters, including but not limited to frequency, duty cycle, and acoustic pressure. In addition, the properties

of stimulated tumor tissues were found, focusing on the elastic modulus as a characterizing parameter of stiffness. The aim is to derive replicable stimulation values, trying to give direction to this area of research.

## 2. Methods

The chosen eligibility criterion was to select research activities whose focus was on sonoporation combined with the penetration of specific drugs or antibodies, relying mainly on article collection platforms, such as PubMed and Scopus. The parameters obtained from the literature are presented here in summary tables reported in the Section 3 named Result. The columns of the following tables are divided by the treated cell lines, and the rows are divided by the parameters: frequency, acoustic pressure, ISPTA, and duty cycle. The type of ultrasonic transducer used is also reported, where it is obtainable from the articles considered. Experimentally, ISPTA can be calculated as the product of ISATA and the ratio of ISP to ISA, indicating thermal effects.

- Intensity spatial average-temporal average (*ISATA*) is the ratio of time-averaged intensity to transducer surface area;
- Intensity spatial peak (*ISP*) denotes the intensity peak measured on the center axis of the single hemicycle of the wave;
- Intensity spatial average (*ISA*) indicates the average intensity of the beam.

The algebraic steps are presented below:

$$ISPTA = ISATA \cdot \frac{ISP}{ISA} = \frac{ISA}{A} \cdot \frac{ISP}{ISA} = \frac{ISP}{A} \quad (1)$$

where  $A$  is defined as the active area of the ultrasonic transducer and corresponds to the surface area of the crystal that emits and receives ultrasound waves (Figure 1).

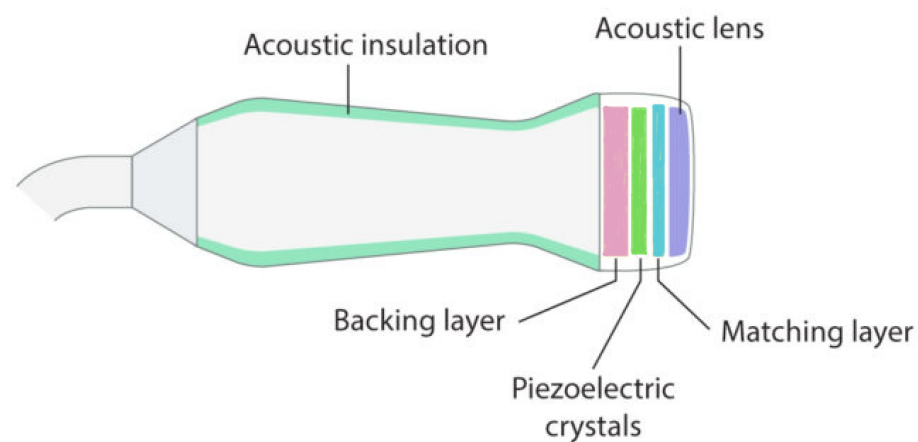


**Figure 1.** Side view of an ultrasonic probe where the piezoelectric crystal coincides with the active area of the transducer.

To calculate *ISP*, the formula referring to the mean value of the acoustic intensity is used, but using the maximum acoustic pressure ( $P$ ), which is obtainable from the probe characterization curves.

$$ISP = \frac{P^2}{2Z} = \frac{P^2}{2\rho c} \quad (2)$$

where  $Z$  is the acoustic impedance,  $\rho$  is the resistivity of the tissue (whose unit of measurement is  $\Omega \cdot m$ ), and  $c$  is the speed of the ultrasonic beam in the transmission medium under consideration.

### 3. Results

The fields of application of this therapy concern different medical districts, such as the liver, colon, prostate, skeletal system, breast, and pancreas. A total of 13 articles were derived in relation to the subject matter, and of these, 32% refer to monolayer tissues and the remaining 68% refer to 3D solid tumors developed by inoculation in the animal model. The graph (Figure 2) presents the breakdown by sonoporation verification techniques found in the articles considered.

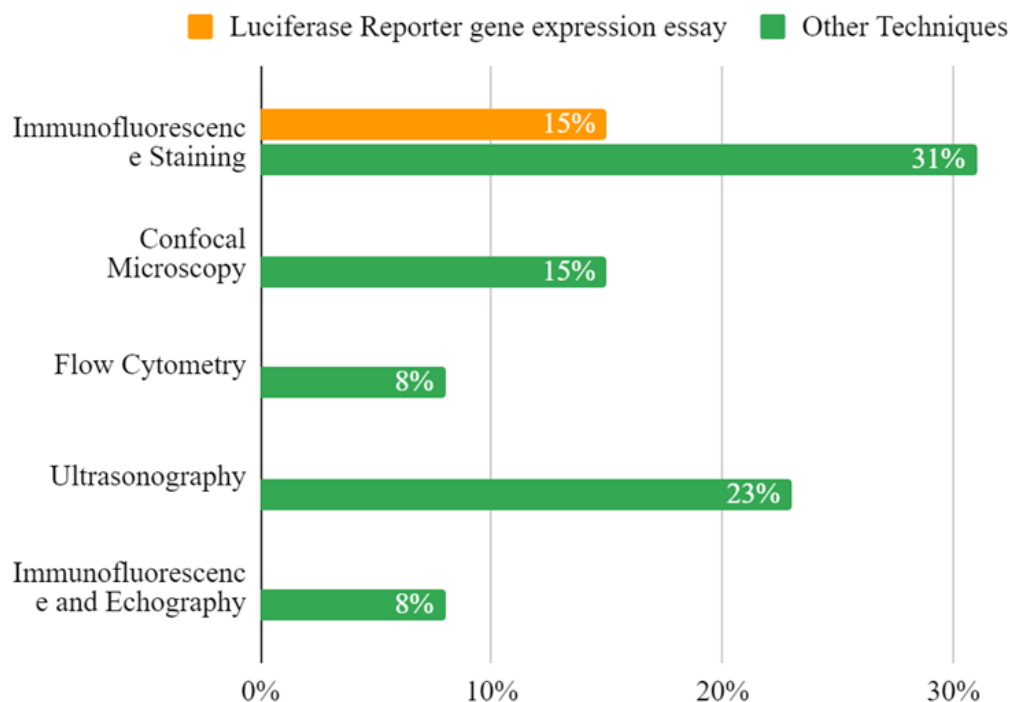


**Figure 2.** The graph represents how sonoporation is verified. In the immunofluorescence bar, 15% shows a different color (orange), as it was possible to extract from the bibliography the use of the luciferase reporter gene expression assay.

#### 3.1. Transducer Classification and Placement in Experimental Setups

Information regarding the transducers used in the selected papers in this review can be found in the table in Section 3 named Result. In addition, some of the reported papers use ultrasonography as a sonoporation verification technique (see Figure 2), so in these cases, the ultrasonography traducers are reported in the tables previously mentioned. However, with some types of devices, such as VEXO2100 (Fujifilm), it is possible to include them in the same verification device settings to initiate a sonoporation process. Regarding the in vitro experiments, it is possible, by means of the identification abbreviations given in the sumary tables presented in the Section 3 named Result, to derive information about each device. The coupling between the transducers and the stimulated cells in the in vivo tests is always performed by means of an aqueous or gel-like medium that allows proper coupling between the ultrasound transducer and the plate or multiwell containing the biological cultures [2]. Where in vivo tests have been conducted, the relative positioning of the transducer with respect to the mouse is associated with a number of related issues:

- The correct coupling between the transducer and the mouse body, taking into account that the mouse body will have curves.
- A waveguide should be constructed to ensure the correct acoustic intensity in the area.
- The reduced surface of the mouse body to be treated.

An interesting approach to the problems in this paragraph is reported in an article [11] that is totally focused on the realization of an experimental setup as shown in Figure 3.

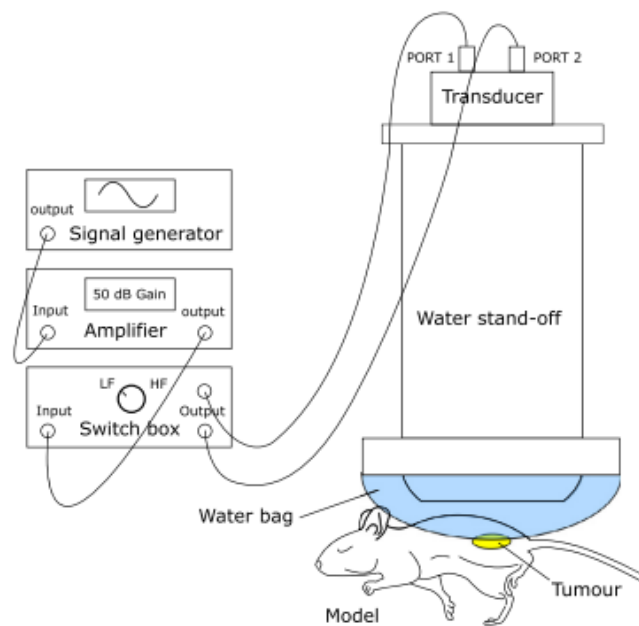


**Figure 3.** Illustration of an experimental setup designed to fit the body of the mouse. Images from [11].

In the subsequent analysis of the results, when considering *in vivo* testing, an explanation of how the coupling takes place between the mouse and the transducer will also be reported.

### 3.2. Analysis of Results by Body District

The following paragraphs list selected articles in the literature by body districts and provide a brief explanation of the content, highlighting innovative aspects.

#### 3.2.1. Colon

In 2012, Zhang et al. conducted a study [12] using a mouse model of human colon cancer. They employed ultrasonic cavitation with specific parameters (238 kHz, 0.5 MPa, 60-s sonication, and a 50% duty cycle) in conjunction with the anti-angiogenic drug, Endostar-MB. Endostar was attached to streptavidin-coated microbubbles, and the study focused on HT29 cells. A custom-built probe was used for ultrasonic cavitation, and contrast-enhanced ultrasound imaging assessed changes in tumor blood flow. The findings indicated that this approach significantly inhibited tumor blood flow, promoted apoptosis, and showcased promise for colon cancer treatment. Unfortunately, this study does not report enough transducer information to derive ISPTA. The Loria et al., (2019) [13] study applied very low-intensity ultrasound (VLIUS) to tumor and normal cells, revealing that a specific VLIUS intensity ( $120 \text{ mW/cm}^2$ ) significantly enhanced the uptake of nanoparticles and improved the delivery of the chemotherapy drug trabectedin in cancer cells. The study potentially offers a promising strategy for targeting colon cancer cells (HT29, HCT116) in a selective way. In the case of Loria and colleagues' study, the acoustic intensity ISPTA threshold was below the cavitation level; this is important to underline and represents an important and innovative approach to the matter. In Nittayacharn et al.'s 2019 *in vivo* study using a mouse model of colorectal cancer [14], the research explores the potential of doxorubicin-loaded nanoscale bubbles (Dox-NBs) combined with low-frequency ultrasound at 3 MHz to enhance drug delivery, demonstrating improved intracellular uptake and therapeutic efficacy, along with increased drug accumulation and distribution within tumors, offering a promising approach to improving cancer therapy.

### 3.2.2. Liver

In the study of Zhao et al. (2018) [15] nanoparticles loaded with a drug called 10-hydroxycamptothecin (10-HCPT) were developed and modified with hyaluronic acid-mediated cell-penetrating peptides (HA/CPPs) to enhance their targeting abilities. In vivo and in vitro studies with different acoustic settings were conducted. In vitro, the nanoparticles were combined with low-intensity focused ultrasound with a frequency of 1.0 MHz, a duty cycle of 50%, and an acoustic intensity of 2000, 2400, and 2800 mW/cm<sup>2</sup>, whereas in 15 mice bearing tumor xenografts, the LIFU settings were changed regarding the intensity (3200 mW/cm<sup>2</sup>). Recently, in 2023, in the study of Chen et al. [16], low-intensity pulsed ultrasound (frequency 1.0 MHz, duty cycle 50%, intensity 500 mW/cm<sup>2</sup>) in combination with microbubbles (MBs) was employed to enhance the delivery of the drug HCPT. In both in vivo and in vitro studies, the researchers found that this technique effectively reduced liver fibrosis. The study suggests that mechanical forces induced by sonoporation might contribute to the observed therapeutic effects. This approach holds promise for clinical use and requires further investigation.

### 3.2.3. Pancreas

In their 2014 study, Kotopoulos and colleagues [17] aimed to enhance the delivery of gemcitabine to pancreatic tumors by investigating the effect of sonoporation via ultrasound (frequency 1.0 MHz, duty cycle 40%) in an orthotopic xenograft mouse model of pancreatic cancer. Figure 4 demonstrates how, in the experimental setup under examination, the transducer was adapted to the body of the mouse by means of an adapter designed to contain an aqueous medium that conforms to the acoustic intensity and the focal length. The results demonstrated that combining sonoporation with gemcitabine therapy significantly reduced primary tumor volumes and increased median survival by up to 10% when compared to control groups. Building on this work, in 2017, the same research team [18] explored the use of acoustic cluster therapy (ACT<sup>®</sup>, a patented microbubble system that can be loaded with drugs that can be activated via ultrasound stimulation) in combination with paclitaxel to improve the therapeutic efficacy in a pre-clinical pancreatic ductal adenocarcinoma (PDAC) mouse model. The experimental setup is visible in Figure 5, where the ecoguided injection of the drug is also taken. The results showed that ACT<sup>®</sup> with paclitaxel led to transient reductions in tumor volume and a potential mechanism for enhanced therapy. In this second article, it is underscored that the acoustic parameters utilized for ultrasonic stimulation and the formulation of the drug warrant further optimization. This optimization process has the potential to yield even more promising results in the context of enhancing therapeutic outcomes. These studies collectively offer promising approaches for enhancing the treatment of pancreatic cancer, which is known for its high mortality rates and limited treatment options, especially in advanced stages. Finally, in 2022, Ng et al.'s research (Figure 6) provides an overview of the results on PDAC xenograft mouse models with the ACT<sup>®</sup> technique combined with paclitaxel, which provided significant reductions in tumor volume in PDAC cell-line-based mouse xenograft models.

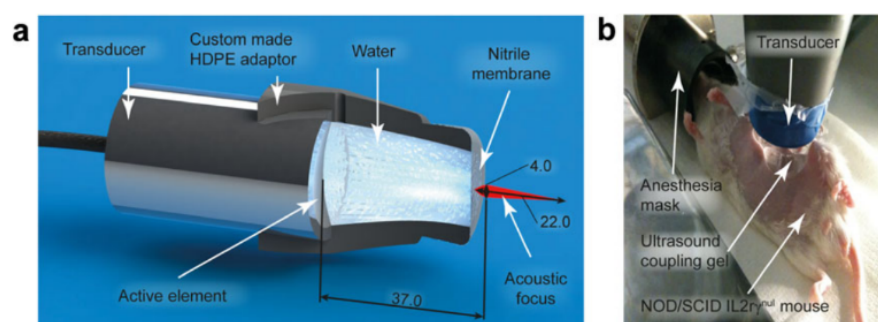


**Figure 4.** Custom-made ultrasound transducer (a). Experimental setup (b). Images from [17].

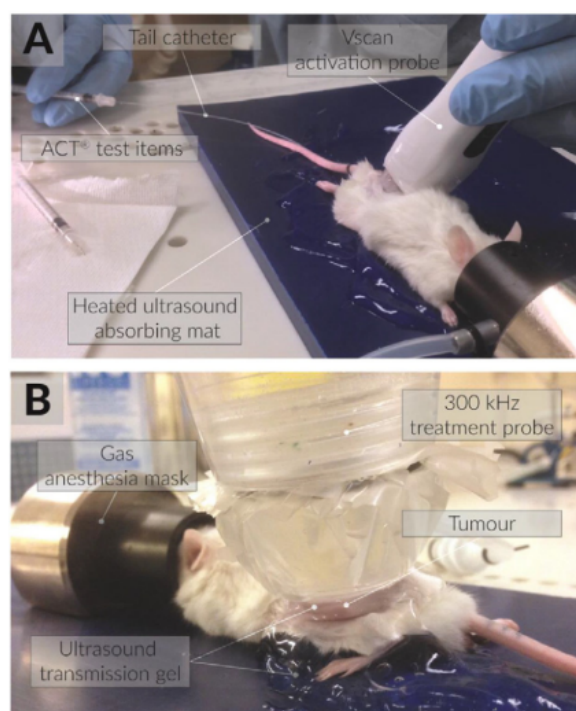


**Figure 5.** Photographs of experimental setup. Mouse undergoing ACT<sup>®</sup> injection (A) and subsequent treatment using the 300 kHz ultrasound probe (B). Images from [18].

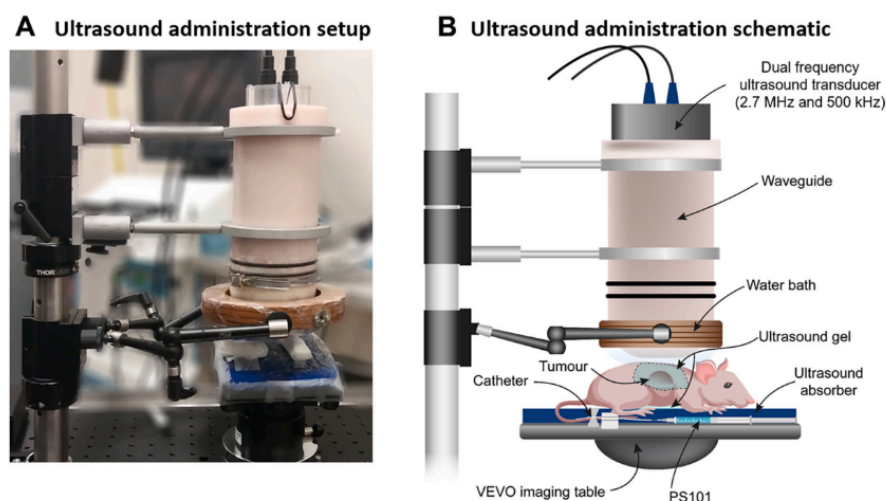


**Figure 6.** Experimental setup from [19] shows a similar approach to [11] with a bag made of plastic material to adapt to the curves of the mouse body. Images from [19].

### 3.2.4. Breast

Zhao et al. [20] (2012) investigated the enhancement of chemotherapeutic-loaded liposomes through acoustic cavitation. They found that doxorubicin-loaded liposomes (DOX liposomes) combined with acoustic cavitation effectively inhibited tumor growth in both in vitro and in vivo experiments. Acoustic cavitation improved the absorption efficiency of DOX liposomes, offering the potential to reduce adverse effects in clinical chemotherapy. The results demonstrated that low-frequency insonation of microbubbles enhanced the uptake of larger molecules while minimizing cancer cell viability. In [21] (2020), Bush et al. investigated the therapeutic efficacy of ACT<sup>®</sup> (as shown in Figure 7), as in [18,19], with liposomal doxorubicin for the treatment of triple negative breast cancer using orthotopic human tumor xenografts (MDA-MB-231-H.luc) in athymic mice (ICR-

NCr-Foxn1nu). The results showed that combining ACT<sup>®</sup> with liposomal doxorubicin improved the absorption of the drug and, consequently, a remission of the mass.

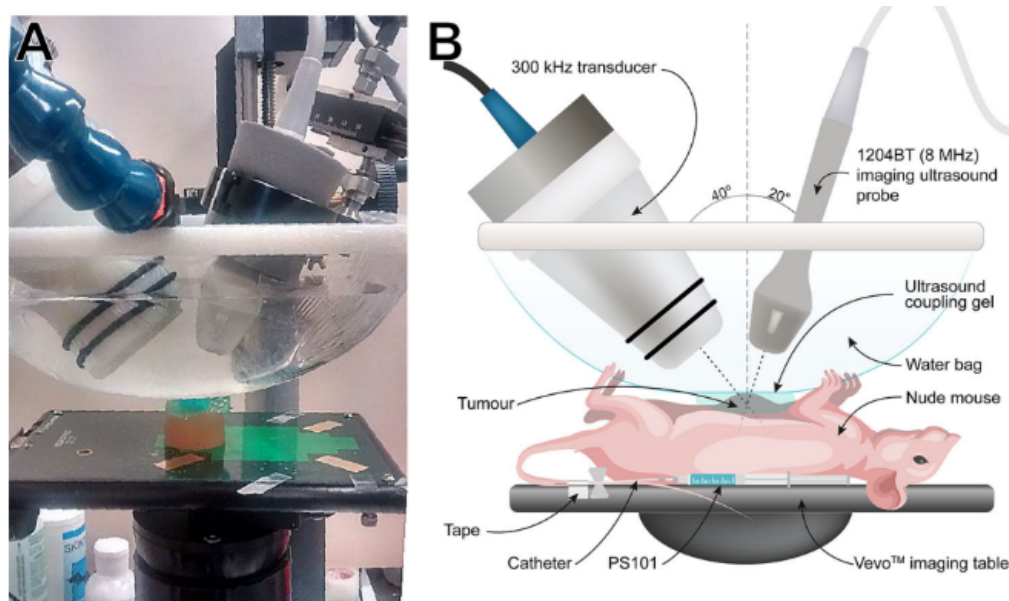


**Figure 7.** In (A) the two probes for stimulation and diagnostics are shown. The mouse is to be placed under the water tank that allows coupling with the transducer. (B) An illustrative reproduction of the instrumentation shown in section A is presented with the mouse under the water tank on the Vevo imaging tank. Images from [21].

More recently, in 2022, Eck et al. [22] explored the use of low-frequency (250 kHz) microbubble-mediated sonoporation for the efficient delivery of molecules with varying sizes in 4T1-type cells that were murine tumor-derived. They optimized the ultrasound parameters and found that an optimal peak negative pressure (PNP) of 500 kPa was crucial for maximizing cell uptake of different-sized molecules, ranging from 1.2 kDa to 70 kDa.

### 3.2.5. Prostate

In 2007, Duvshani-Eshet et al. demonstrated the effectiveness of sonoporation, in non-viral gene delivery to prostate tumors. Their study successfully transfected prostate cancer cells and endothelial cells *in vitro*, showcasing significant inhibition of EC migration and proliferation. *In vivo*, the research led to substantial tumor growth inhibition. It is necessary to specify that, in this case, genes are discussed as molecules that penetrate the membrane. This is why they have been included in the review, even though it does not specifically address bubbles encapsulating drugs or drugs themselves. In Wang et al. [23] (2012), the combination therapy involving low-frequency and low-intensity ultrasound along with microbubbles (UM) was explored for the targeted delivery of mitoxantrone HCl (MIT) to DU145 cells, which are known for their drug-resistant nature. The results demonstrated that this approach significantly improved drug uptake and therapeutic efficacy without impacting cell viability. Furthermore, the treatment exhibited notable effects on the migration capability of DU145 cells. Overall, the ultrasonic parameters (frequency, 21 kHz; power density, 2 min at a duty cycle of 70%) used in this research hold promise for enhancing chemotherapeutic outcomes while mitigating MIT's adverse side effects. It is important to note that ultrasound-mediated microbubble therapy has broader applications in cancer treatment and is particularly relevant in addressing the challenges posed by prostate cancer.

### 3.2.6. Bone

A unique research study conducted by Shar B.S. et al. (2022) [24] aimed at developing, optimizing, and testing an ultrasound-responsive targeted nanodroplet system for delivering Cathepsin K small interfering RNA (CTSK siRNA) as a potential treatment for osteoporosis. Specifically, ultrasound was utilized at 1MHz in this instance.

### 3.2.7. Ovaries

In the study of Suzuki et al. (2010) [25], a combination of ultrasound and innovative ultrasound-sensitive liposomes was employed to enhance interleukin-12 (IL-12) gene therapy for cancer, as in [26]. An impactful and noteworthy study by Pu et al. (2014) [27] developed LHRH receptor-targeted and paclitaxel-loaded lipid microbubbles (TPLMBs) to enhance chemotherapy delivery in ovarian cancer treatment. In an ovarian cancer model, TPLMBs effectively bound to tumor cells, and ultrasound-mediated destruction of these microbubbles resulted in significantly improved therapeutic outcomes, including increased tumor apoptosis and reduced angiogenesis. The findings indicate that ultrasound-mediated intraperitoneal administration of targeted drug-loaded microbubbles holds promise for ovarian cancer treatment. Furthermore, it is worth noting that the stimulation in this case occurred at low frequencies, approximately 300 KHz. All the parameters obtained from the bibliography are reported in summary tables (Tables 1–8). One important parameter in US is the acoustic intensity, which, in this review, is expressed as ISPTA, as in most of the scientific literature on sonoporation. Compared to the application of diagnostic imaging, which applies ultrasound at intensities ranging from 0.05 to 0.5 W/cm<sup>2</sup>, the application of ultrasound in surgery involves high intensities of 0.2–100 W/cm<sup>2</sup> and up to 10,000 W/cm<sup>2</sup>. The use of therapeutic ultrasound ranges from high to low intensities. Thermal effects predominate in the former, and non-thermal effects, such as cavitation and transfer of drug, in the latter. Low-intensity US can be further subdivided into pulsed and continuous US, depending on the duty cycle. Pulsed US is characterized by ON/OFF cycles, while continuous US has a duty cycle of 100%. A new frontier to improve delivery to tumor cells could be the use of very low-intensity ultrasound (VLIUS), at intensities lower than 120 mW/cm<sup>2</sup> [13]. These would further reduce the generation of significant amounts of heat that would damage tissues and cells. By integrating the information from the elastic modulus and acoustic pressure tables, where both values were present, it was not possible to identify a correlation. However, this could be linked to the different study approaches and sample selection. Solid tumors present interesting characteristics that differentiate them from their surrounding environment. Palpation often serves as the initial diagnostic method, as tumors exhibit greater rigidity than their surroundings.

At the cellular level, individual cancer cells appear to be softer and even more deformable than their healthy counterparts. Cancer cells undergo changes throughout the progression of the disease, acquiring biological properties not present in normal cells, such as the ability to replicate indefinitely [28]. One of the most remarkable phenomena associated with cancer is metastatic spreading. This leads to the formation of secondary tumors in distant organs, far away from the primary tumor site. The process involves cancer cells invading the bloodstream (intravasation) and then exiting the blood vessels to establish new tumors (extravasation). Research has revealed an essential aspect of tumor development: the role of stroma stiffening. Stiffening of the surrounding tissue induces tumor rigidity, which, in turn, contributes to tumor progression [29]. Understanding these unique characteristics of cancer cells and the mechanisms behind tumor progression is crucial in developing targeted and effective treatments to combat this disease. A further distinction between healthy and tumor cells is their stiffness, as reported in Table 8. Tumor cells, unlike their healthy counterparts, show a significantly lower elastic rigidity. This specific characteristic is closely linked to the ability of cancer cells to metastasize or spread throughout the body. To determine the elastic modulus of normal and cancer cells and observe how they react to applied forces, researchers often use an atomic force microscope (AFM). With this technique, the mechanical properties of cell surfaces are deformed and

analyzed [30]. Interestingly, the elastic moduli of benign cells show a wider variation, following a log-normal distribution. On the other hand, malignant cells show a much narrower log-normal distribution of elastic rigidity.

**Table 1.** Colon cancer cells.

Parameters	Colon (HT29): Colorectal Adenocarcinoma [12]	Colon (HT29, HCT116): Colorectal Adenocarcinoma [13]	Colon (LS-174T): Colorectal Adenocarcinoma [14]
Probe	Transducer from Haiying Medical Electronic Instrument Company	US transducer 10–100 V	Linear US Probe
Frequency (MHz)	0.238	1	3
Acoustic Pressure (MPa)	0.5	4.3 <sup>1</sup>	-
ISPTA (mW/cm <sup>2</sup> )	-	120	2000
Duty Cycle	0.50	-	0.20

<sup>1</sup> This value was calculated using the inverse Formula (2).

**Table 2.** Liver cancer cells.

Parameters	Liver (SMMC-7721): Hepatocarcinoma [15]	Liver (Hepatic Fibrosis) [16]
Probe	Linear Array Probe	Vevo 2100, MS250 transducer
Frequency (MHz)	1	1
Acoustic Pressure (MPa)	-	-
ISPTA (mW/cm <sup>2</sup> )	2400	500
Duty Cycle	0.50	0.50

**Table 3.** Pancreas cancer cells.

Parameters	PDAC (MIA PaCa-2): Pancreatic Ductal Adenocarcinoma [17]	PDAC (MIA PaCa-2): Pancreatic Ductal Adenocarcinoma [18]	PDAC: Pancreatic Ductal Adenocarcinoma [19]
Probe	Vevo 2100, MS250 transducer	Vevo 2100, MS250 transducer	Custom-made transducer (Relab, Horten, Norway)
Frequency (MHz)	1	0.3	0.5–2.7 MHz
Acoustic Pressure (MPa)	0.2	0.4	-
ISPTA (mW/cm <sup>2</sup> )	688	2.39	-
Duty Cycle	0.40	0.73	-

**Table 4.** Breast cancer cells.

Parameters	4T1: Mammary Carcinoma [22]	MDA-MB-435: Derived from Melanoma Cell Line [20]	MDA-MB-231-Luc TNBC: Derived from Melanoma Cell Line [21]
Probe	Spherically focused single element transducer	CZT-8A sonicator, Xinzheng Company, ShenYang, China	Aplio XG ultrasound scanner (Toshiba Medical Systems Corporation, Tochigi, Japan), 1204BT linear array ultrasound probe
Frequency (MHz)	0.25	1	0.3
Acoustic Pressure (MPa)	0.5	-	-
ISPTA (mW/cm <sup>2</sup> )	-	300	-
Duty Cycle	-	0.5	-

**Table 5.** Prostate cancer cells.

Parameters	DU145: Prostate Adenocarcinoma Origin [23]	LNCaP: Prostate Carcinoma [26]
Probe	FS450 Ultrasonic homogenizer sonicator	UltraMax, XLTEK
Frequency (MHz)	0.021	1
Acoustic Pressure (MPa)	-	-
ISPTA (mW/cm <sup>2</sup> )	113	2000
Duty Cycle	0.7	0.3

**Table 6.** Bone (treatment for osteoporosis).

Parameters	Stimulation of Osteoclast [24]
Probe	Fisherbrand Model 120 Sonic Dismembrator
Frequency (MHz)	1
Acoustic Pressure (MPa)	-
ISPTA (mW/cm <sup>2</sup> )	3000
Duty Cycle	0.5–1

**Table 7.** Ovarian cancer cells.

Parameters	OV-HM: Ovarian Cancer Cells [25]	A2780/DDP: Ovarian Cancer Cells [27]
Probe	-	Model CGZZ, Ultrasonographic Image Research Institute, Chongqing Medical University, China
Frequency (MHz)	1	0.3
Acoustic Pressure (MPa)	-	-
ISPTA (mW/cm <sup>2</sup> )	700	1000
Duty Cycle	-	0.5

**Table 8.** Elastic modulus of the main cell lines mentioned. The variability of values depends on the amount of collagen developed by the tumor.

Cellular Line	Elastic Modulus (kPa)
Colon (HT29) [31]	[5–15]
Colon (HCT116) [31]	[2–70]
Colon (LS174-T) [32]	[0.302–0.566]
Liver (SMMC-7721) [33]	[1.2–1.7]
Liver (hepatic fibrosis) [34]	1.7
Pancreas (MIA PaCa-2) [35]	[0.7–2.7]
Pancreas (PANC-1) [35]	[1.3–3.4]
Breast cancer cell (4T1) [36]	0.45
Breast cancer cell (MDA-MB-435) [37]	[12–22]
Prostate cancer cell (DU145) [38]	[0.2–0.8]
Prostate cancer cell (LNCaP) [39]	[0.235–0.339]
Bone (osteoclast)	-
Ovarian cancer cell (OV-HM)	-
Ovarian cancer cell (A2780/DDP)	-

By integrating the information from the tables of elastic moduli and acoustic intensities, pressure, and frequency, a graph was drawn with the concentration of the items by body district. The reason for this grouping is related to the need to identify in which body districts the parameters are concentrated in order to give a guide to those who would like to approach this type of research and experimentation in the future with a background of what has been performed on that organ in the past. However, a close correlation is not expected due to the different study approaches and sample selection, considering the

difference between a monolayer tissue and a tumor spheroid, where drug penetration is slowed down by aggregation between cells. In addition, some of these studies were conducted *in vivo*. In these cases, the treatment of the tumor mass *in vivo* follows the growth of an inoculated tumor mass in the animal model.

Nevertheless, it is conceivable that an effort in the direction of data standardization could give further impetus to research.

#### 4. Discussion and Conclusions

The present paper provides a thorough analysis of the available literature regarding the possible application of sonoporation for a novel therapeutic strategy in cancer treatment, analyzing the available data relative to the preclinical application of sonoporation in different cancer types and different cancer models.

However, it is necessary to point out the main challenges and limitations inherent in this issue:

- Ultrasound, especially at high acoustic intensities, can induce collateral damages that are not easy to predict; this is why low-intensity applications must be promoted.
- The penetration capability of ultrasounds depends on the frequency adopted for the treatment. This leads to technical difficulties related to the need to adapt the experimental setups in relation to frequency, resulting in different configurations of the relative position between the probe and the sample. Sonoporation has a limitation in specificity, as it can cause undesired effects in neighboring cells. Consequently, it is imperative to further investigate the intensities and frequencies used in sonoporation in order to achieve an optimal compromise between the effectiveness of stimulation and the mitigation of potential damage to healthy cells.

Moreover, there is a low correlation between elastic modules and acoustic intensity, pressure, and frequency, as shown in the graphs in Figure 8–10, respectively. A considerable variability in the data collected is evident; however, it is important to emphasize that this lack of correlation is due to substantial differences in the study protocols adopted. As reported in the results, some of the articles are based on *in vivo* models while others are based on *in vitro* models, and some use three-dimensional tissues and others use single-layered tissues. These methodological differences may lead to apparently conflicting results but instead represent the different applications of a complex phenomenon.

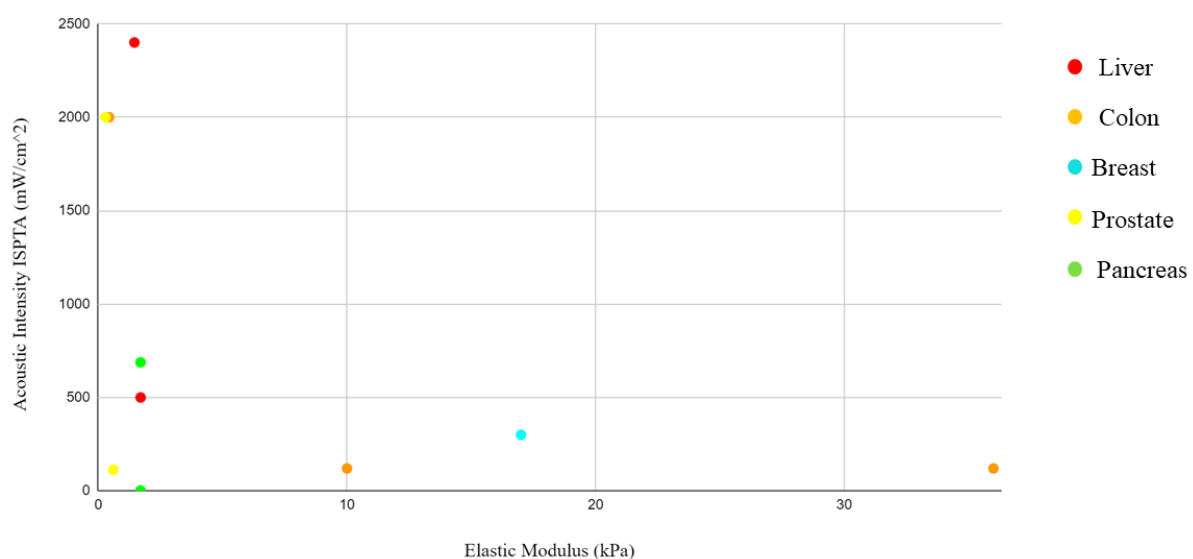


**Figure 8.** Acoustic intensity related to elastic modulus.

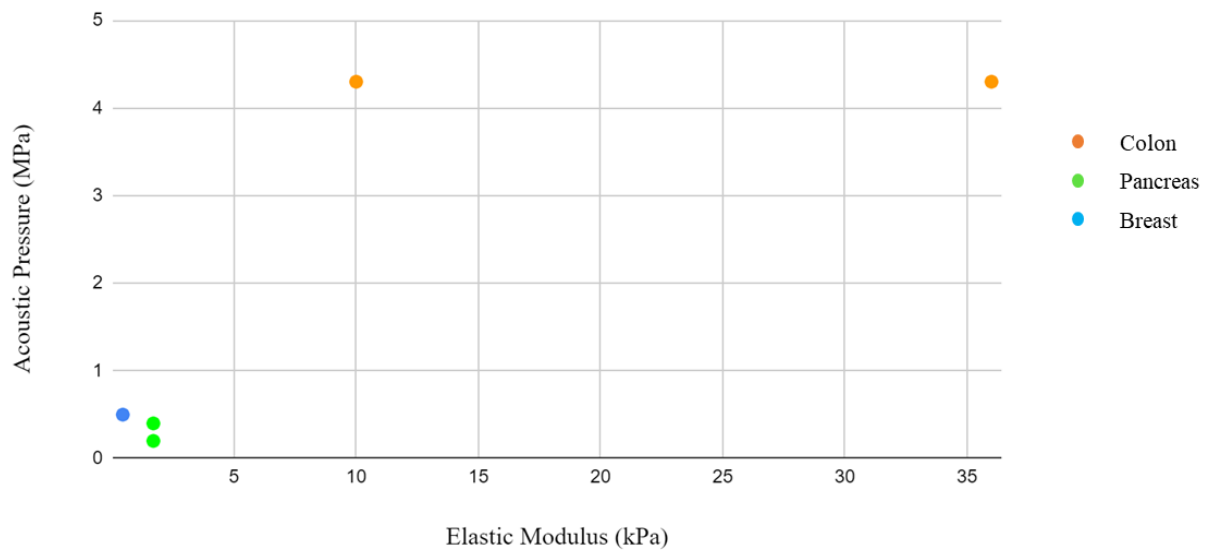


**Figure 9.** Acoustic pressure related to elastic modulus.

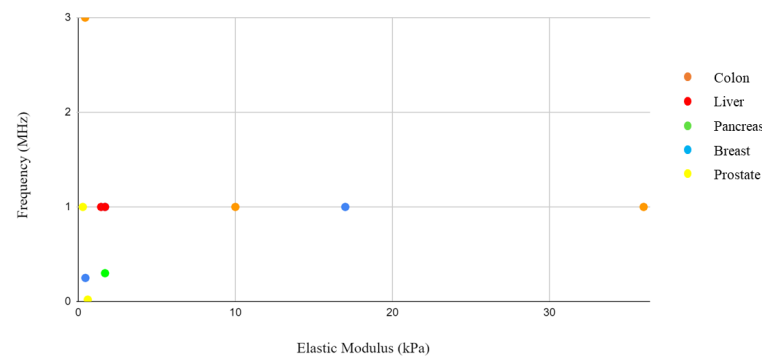


**Figure 10.** Frequency related to elastic modulus.

The authors of this paper argue for the need to characterize in depth the fundamental mechanical variables that describe both 2D single-layer cells and 3D cultures. It is important to note that the latter may not exhibit the same mechanical behavior as the former. This in-depth study is crucial to establish an effective correlation between the stiffness of the stimulated sample and the applied intensity. In particular, the characterization of Young's modulus, stress–strain curves, and resonance frequency emerge as relevant aspects.

The determination of Young's modulus for three-dimensional cultures, which, by their nature, are immersed in multiwell containers rather than on slides or plates, presents considerable technical difficulties. The AFM investigation method works relatively well with 2D samples; instead, for the best characterization of mechanical properties of 3D samples [40], the data could undergo a deep analysis with the support of specific software to simulate the complex structure and the interaction between cells and the extracellular matrix.

Furthermore, as far as the resonance frequency is concerned, finding it for cancerous tissue could clarify whether it is close to the stimulation frequencies used to induce the sonoporation phenomenon in the samples. Indeed, it is also possible that these frequencies are correlated with the tissue type, which this analysis would lead us to understand.

Additionally, it is pivotal to highlight the limited number of publications available on this topic of research due to the complexity of sonoporation. The scarcity of scientific literature can be a significant challenge, as it limits access to established knowledge. However, this scarcity also offers a huge opportunity for new discoveries, so it would be interesting to increase the efforts devoted to its analysis. Furthermore, as has emerged from the literature search, there is no unified approach to sonoporation verification, but it would be useful to have a unified validation standard to homogenize procedures and

have more comparable results. In the case of confocal microscopy, for example, for all of the drugs that do not possess intrinsic luminescence, it is necessary to use a marker, whose molar mass is relevant, to verify the entry of the substance to be monitored into the tumor cell. However, immunofluorescence is the most widely used method for testing in vitro sonoporation (Figure 2), while, regarding in vivo experiments, ultrasonography is the most commonly used. This information offers guidance on what is considered to be best practice in the field of sonoporation.

Future perspectives and possible research developments: Sonoporation could offer a valid treatment strategy in combination with drugs, small molecules, or antibody fragments. Such an approach could be an advantage in terms of tissue penetration and targeting, thus representing a valid combined option both for diagnostic and therapeutic applications [41–43]. In particular, the possibility of using sonoporation together with drugs that selectively target cancer cells to increase the effectiveness and non-invasiveness of oncological therapies could represent a significant step forward in the translation of cancer research to the clinical setting. Finally, it would be relevant to move from in vitro monolayer testing to a three-dimensional cell and tissue culture system before going to the in vivo phase of animal experimentation. This has the aim of reducing the suffering of animals and refining the effectiveness of penetration in a tissue, in accordance with the principles of the three Rs.

**Author Contributions:** Conceptualization, M.R. and E.B.; methodology, M.D.; validation, C.D.; writing—original draft preparation, E.B.; writing—review and editing, M.R.; visualization, M.R.; supervision, A.C.; correspondence, A.A. All authors have read and agreed to the published version of the manuscript.

**Funding:** This research received no external funding.

**Data Availability Statement:** Not applicable.

**Acknowledgments:** The authors extend sincere gratitude to Tiziano Lottini for his technical and professional support.

**Conflicts of Interest:** The authors declare no conflicts of interest.

### Abbreviations

The following abbreviations are used in this manuscript:

US	Ultrasound
ISPTA	Intensity spatial peak temporal average
LICU	Low-intensity continuous ultrasound
LIPUS	Low-intensity pulsed ultrasound
HIFU	High-intensity continuous ultrasound

### References

1. Lottini, T.; Buonamici, M.; Duranti, C.; Arcangeli, A. Generation of an Orthotopic Xenograft of Pancreatic Cancer Cells by Ultrasound-Guided Injection. *JoVE (J. Vis. Exp.)* **2021**, *177*, e63123.
2. Dimitri, M.; Duranti, C.; Aquino, S.; Mazzantini, L.; Iorio, J.; Lulli, M.; Ricci, M.; Capineri, L.; Arcangeli, A.; Corvi, A. Biophysical and Biomechanical Effect of Low Intensity US Treatments on Pancreatic Adenocarcinoma 3D Cultures. *Appl. Sci.* **2022**, *12*, 666. [[CrossRef](#)]
3. Bazou, D.; Maimon, N.; Munn, L.L.; Gonzalez, I. Effects of low intensity continuous ultrasound (LICU) on mouse pancreatic tumor explants. *Appl. Sci.* **2017**, *7*, 1275. [[CrossRef](#)]
4. Ikeda, T.; Yoshizawa, S.; Koizumi, N.; Mitsuishi, M.; Matsumoto, Y. Focused ultrasound and lithotripsy. In *Therapeutic Ultrasound*; Springer: Berlin/Heidelberg, Germany, 2016; pp. 113–129.
5. Yoshizawa, S.; Ikeda, T.; Ito, A.; Ota, R.; Takagi, S.; Matsumoto, Y. High intensity focused ultrasound lithotripsy with cavitating microbubbles. *Med. Biol. Eng. Comput.* **2009**, *47*, 851–860. [[CrossRef](#)] [[PubMed](#)]
6. Delalande, A.; Kotopoulis, S.; Rovers, T.; Pichon, C.; Postema, M. Sonoporation at a low mechanical index. *Bubble Sci. Eng. Technol.* **2011**, *3*, 3–12. [[CrossRef](#)]
7. Fan, Z.; Kumon, R.E.; Deng, C.X. Mechanisms of microbubble-facilitated sonoporation for drug and gene delivery. *Ther. Deliv.* **2014**, *5*, 467–486. [[CrossRef](#)] [[PubMed](#)]

8. Feril, L.B.; Tachibana, K.; Ogawa, K.; Yamaguchi, K.; Solano, I.G.; Irie, Y. Therapeutic potential of low-intensity ultrasound (part 1): Thermal and sonomechanical effects. *J. Med. Ultrason.* **2008**, *35*, 153–160. [[CrossRef](#)] [[PubMed](#)]
9. O'Brien, W.D., Jr. Ultrasound–biophysics mechanisms. *Prog. Biophys. Mol. Biol.* **2007**, *93*, 212–255. [[CrossRef](#)]
10. Deng, C.X.; Sieling, F.; Pan, H.; Cui, J. Ultrasound-induced cell membrane porosity. *Ultrasound Med. Biol.* **2004**, *30*, 519–526. [[CrossRef](#)]
11. Andersen, K.K.; Healey, A.; Bush, N.L.; Frijlink, M.E.; Hoff, L. A harmonic dual-frequency transducer for acoustic cluster therapy. *Ultrasound Med. Biol.* **2019**, *45*, 2381–2390. [[CrossRef](#)]
12. Zhang, C.; Huang, P.; Zhang, Y.; Chen, J.; Shentu, W.; Sun, Y.; Yang, Z.; Chen, S. Anti-tumor efficacy of ultrasonic cavitation is potentiated by concurrent delivery of anti-angiogenic drug in colon cancer. *Cancer Lett.* **2014**, *347*, 105–113. [[CrossRef](#)] [[PubMed](#)]
13. Loria, R.; Giliberti, C.; Bedini, A.; Palomba, R.; Caracciolo, G.; Ceci, P.; Falvo, E.; Marconi, R.; Falcioni, R.; Bossi, G.; et al. Very low intensity ultrasounds as a new strategy to improve selective delivery of nanoparticles-complexes in cancer cells. *J. Exp. Clin. Cancer Res.* **2019**, *38*, 1. [[CrossRef](#)] [[PubMed](#)]
14. Nittayacharn, P.; Yuan, H.X.; Hernandez, C.; Bielecki, P.; Zhou, H.; Exner, A.A. Enhancing tumor drug distribution with ultrasound-triggered nanobubbles. *J. Pharm. Sci.* **2019**, *108*, 3091–3098. [[CrossRef](#)]
15. Zhao, H.; Wu, M.; Zhu, L.; Tian, Y.; Wu, M.; Li, Y.; Deng, L.; Jiang, W.; Shen, W.; Wang, Z.; et al. Cell-penetrating peptide-modified targeted drug-loaded phase-transformation lipid nanoparticles combined with low-intensity focused ultrasound for precision theranostics against hepatocellular carcinoma. *Theranostics* **2018**, *8*, 1892. [[CrossRef](#)] [[PubMed](#)]
16. Chen, Q.; Huang, J.; Ye, Y.; Hu, A.; Xu, B.; Hu, D.; Wang, L.; Xing, L.; Chen, S.; Gui, X.; et al. Delivery of hydroxycamptothecin via sonoporation: An effective therapy for liver fibrosis. *J. Control. Release* **2023**, *358*, 319–332. [[CrossRef](#)] [[PubMed](#)]
17. Kotopoulis, S.; Delalande, A.; Popa, M.; Mamaeva, V.; Dimceviski, G.; Gilja, O.H.; Postema, M.; Gjertsen, B.T.; McCormack, E. Sonoporation-enhanced chemotherapy significantly reduces primary tumour burden in an orthotopic pancreatic cancer xenograft. *Mol. Imaging Biol.* **2014**, *16*, 53–62. [[CrossRef](#)] [[PubMed](#)]
18. Kotopoulis, S.; Stigen, E.; Popa, M.; Safont, M.M.; Healey, A.; Kvåle, S.; Sontum, P.; Gjertsen, B.T.; Gilja, O.H.; McCormack, E. Sonoporation with Acoustic Cluster Therapy (ACT®) induces transient tumour volume reduction in a subcutaneous xenograft model of pancreatic ductal adenocarcinoma. *J. Control. Release* **2017**, *245*, 70–80. [[CrossRef](#)]
19. Ng, S.; Healey, A.J.; Sontum, P.C.; Kvåle, S.; Torp, S.H.; Sulheim, E.; Von Hoff, D.; Han, H. Effect of acoustic cluster therapy (ACT®) combined with chemotherapy in a patient-derived xenograft mouse model of pancreatic cancer. *J. Control. Release* **2022**, *352*, 1134–1143. [[CrossRef](#)]
20. Zhao, Y.Z.; Dai, D.D.; Lu, C.T.; Lv, H.F.; Zhang, Y.; Li, X.; Li, W.F.; Wu, Y.; Jiang, L.; Li, X.K.; et al. Using acoustic cavitation to enhance chemotherapy of DOX liposomes: experiment in vitro and in vivo. *Drug Dev. Ind. Pharm.* **2012**, *38*, 1090–1098. [[CrossRef](#)]
21. Bush, N.; Healey, A.; Shah, A.; Box, G.; Kirkin, V.; Eccles, S.; Sontum, P.C.; Kotopoulis, S.; Kvåle, S.; van Wamel, A.; et al. Theranostic attributes of acoustic cluster therapy and its use for enhancing the effectiveness of liposomal doxorubicin treatment of human triple negative breast cancer in mice. *Front. Pharmacol.* **2020**, *11*, 75. [[CrossRef](#)]
22. Eck, M.; Aronovich, R.; Ilovitsh, T. Efficacy optimization of low frequency microbubble-mediated sonoporation as a drug delivery platform to cancer cells. *Int. J. Pharm.* **2022**, *4*, 100132. [[CrossRef](#)] [[PubMed](#)]
23. Wang, Y.; Bai, W.K.; Shen, E.; Hu, B. Sonoporation by low-frequency and low-power ultrasound enhances chemotherapeutic efficacy in prostate cancer cells in vitro. *Oncol. Lett.* **2013**, *6*, 495–498. [[CrossRef](#)] [[PubMed](#)]
24. Shar, A.; Aboutalebianaraki, N.; Misiiti, K.; Sip, Y.Y.L.; Zhai, L.; Razavi, M. A novel ultrasound-mediated nanodroplet-based gene delivery system for osteoporosis treatment. *Nanomed. Nanotechnol. Biol. Med.* **2022**, *41*, 102530. [[CrossRef](#)] [[PubMed](#)]
25. Suzuki, R.; Namai, E.; Oda, Y.; Nishiie, N.; Otake, S.; Koshima, R.; Hirata, K.; Taira, Y.; Utoguchi, N.; Negishi, Y.; et al. Cancer gene therapy by IL-12 gene delivery using liposomal bubbles and tumoral ultrasound exposure. *J. Control. Release* **2010**, *142*, 245–250. [[CrossRef](#)]
26. Duvshani-Eshet, M.; Benny, O.; Morgenstern, A.; Machluf, M. Therapeutic ultrasound facilitates antiangiogenic gene delivery and inhibits prostate tumor growth. *Mol. Cancer Ther.* **2007**, *6*, 2371–2382. [[CrossRef](#)] [[PubMed](#)]
27. Pu, C.; Chang, S.; Sun, J.; Zhu, S.; Liu, H.; Zhu, Y.; Wang, Z.; Xu, R.X. Ultrasound-mediated destruction of LHRHa-targeted and paclitaxel-loaded lipid microbubbles for the treatment of intraperitoneal ovarian cancer xenografts. *Mol. Pharm.* **2014**, *11*, 49–58. [[CrossRef](#)]
28. Alibert, C.; Goud, B.; Manneville, J.B. Are cancer cells really softer than normal cells? *Biol. Cell* **2017**, *109*, 167–189. [[CrossRef](#)]
29. Levental, K.R.; Yu, H.; Kass, L.; Lakins, J.N.; Egeblad, M.; Erler, J.T.; Fong, S.F.; Csiszar, K.; Giaccia, A.; Werninger, W.; et al. Matrix crosslinking forces tumor progression by enhancing integrin signaling. *Cell* **2009**, *139*, 891–906. [[CrossRef](#)]
30. Suresh, S. Elastic clues in cancer detection. *Nat. Nanotechnol.* **2007**, *2*, 748–749. [[CrossRef](#)]
31. Liu, C.; Pei, H.; Tan, F. Matrix stiffness and colorectal cancer. *Oncotargets Ther.* **2020**, *13*, 2747–2755. [[CrossRef](#)]
32. Mills, K.; Garikipati, K.; Kemkemer, R. Experimental characterization of tumor spheroids for studies of the energetics of tumor growth. *Int. J. Mater. Res.* **2011**, *102*, 889–895. [[CrossRef](#)]
33. Zhu, X.; Wang, Z.; Liu, X. Investigation of effect of fullerene on viscoelasticity properties of human hepatocellular carcinoma by AFM-based creep tests. *J. Mater. Res.* **2017**, *32*, 2521–2531. [[CrossRef](#)]
34. Yeh, W.C.; Li, P.C.; Jeng, Y.M.; Hsu, H.C.; Kuo, P.L.; Li, M.L.; Yang, P.M.; Lee, P.H. Elastic modulus measurements of human liver and correlation with pathology. *Ultrasound Med. Biol.* **2002**, *28*, 467–474. [[CrossRef](#)] [[PubMed](#)]

35. Nguyen, A.V.; Nyberg, K.D.; Scott, M.B.; Welsh, A.M.; Nguyen, A.H.; Wu, N.; Hohlbauch, S.V.; Geisse, N.A.; Gibb, E.A.; Robertson, A.G.; et al. Stiffness of pancreatic cancer cells is associated with increased invasive potential. *Integr. Biol.* **2016**, *8*, 1232–1245. [[CrossRef](#)] [[PubMed](#)]
36. Qiu, S.; Zhao, X.; Chen, J.; Zeng, J.; Chen, S.; Chen, L.; Meng, Y.; Liu, B.; Shan, H.; Gao, M.; et al. Characterizing viscoelastic properties of breast cancer tissue in a mouse model using indentation. *J. Biomech.* **2018**, *69*, 81–89. [[CrossRef](#)] [[PubMed](#)]
37. Li, Q.; Xiao, L.; Harihar, S.; Welch, D.R.; Vargis, E.; Zhou, A. In vitro biophysical, microspectroscopic and cytotoxic evaluation of metastatic and non-metastatic cancer cells in responses to anti-cancer drug. *Anal. Methods* **2015**, *7*, 10162–10169. [[CrossRef](#)] [[PubMed](#)]
38. Efremov, Y.M.; Dokrunova, A.; Efremenko, A.; Kirpichnikov, M.; Shaitan, K.; Sokolova, O. Distinct impact of targeted actin cytoskeleton reorganization on mechanical properties of normal and malignant cells. *Biochim. Biophys. Acta-(Bba)-Mol. Cell Res.* **2015**, *1853*, 3117–3125. [[CrossRef](#)]
39. Faria, E.C.; Ma, N.; Gazi, E.; Gardner, P.; Brown, M.; Clarke, N.W.; Snook, R.D. Measurement of elastic properties of prostate cancer cells using AFM. *Analyst* **2008**, *133*, 1498–1500. [[CrossRef](#)]
40. Guillaume, L.; Rigal, L.; Fehrenbach, J.; Severac, C.; Ducommun, B.; Lobjois, V. Characterization 525 of the physical properties of tumor-derived spheroids reveals critical insights for pre-clinical 526 studies. *Sci. Rep.* **2019**, *9*, 6597. [[CrossRef](#)]
41. Duranti, C.; Lastraioli, E.; Iorio, J.; Capitani, C.; Carraresi, L.; Gonnelli, L.; Arcangeli, A. Expression and purification of a novel single-chain diabody (scDb-hERG1/ $\beta$ 1) from *Pichia pastoris* transformants. *Protein Expr. Purif.* **2021**, *184*, 105879. [[CrossRef](#)]
42. Duranti, C.; Iorio, J.; Lottini, T.; Lastraioli, E.; Crescioli, S.; Bagni, G.; Lulli, M.; Capitani, C.; Bouazzi, R.; Stefanini, M.; et al. Harnessing the hERG1/ $\beta$ 1 integrin complex via a novel bispecific single-chain antibody: An effective strategy against solid cancers. *Mol. Cancer Ther.* **2021**, *20*, 1338–1349. [[CrossRef](#)] [[PubMed](#)]
43. Duranti, C.; Iorio, J.; Bagni, G.; Altadonna, G.C.; Fillion, T.; Lulli, M.; D'Alessandro, F.N.; Montalbano, A.; Lastraioli, E.; Fanelli, D.; et al. Integrins regulate hERG1 dynamics by girdin-dependent  $G\alpha i3$ : signaling and modeling in cancer cells. *Life Sci. Alliance* **2024**, *7*, e202302135. [[CrossRef](#)] [[PubMed](#)]

**Disclaimer/Publisher's Note:** The statements, opinions and data contained in all publications are solely those of the individual author(s) and contributor(s) and not of MDPI and/or the editor(s). MDPI and/or the editor(s) disclaim responsibility for any injury to people or property resulting from any ideas, methods, instructions or products referred to in the content.